Spectral Linewidth vs. Front Facet Reflectivity of 780 nm DFB Diode Lasers at High Optical Output Power

Thanh-Phuong Nguyen [1,*], Hans Wenzel [2], Olaf Brox [2], Frank Bugge [2], Peter Ressel [2], Max Schiemangk [2], Andreas Wicht [2], Tran Quoc Tien [3] and Günther Tränkle [2]

[1]   School of Engineering Physics, Hanoi University of Science and Technology, No. 1 Dai Co Viet, Hai Ba Trung, Hanoi, Vietnam

[2]   Ferdinand-Braun-Institut, Gustav-Kirchhoff-Str. 4, 12489 Berlin, Germany; hans.wenzel@fbh-berlin.de (H.W.); olaf.brox@fbh-berlin.de (O.B.); frank.bugge@fbh-berlin.de (F.B.); peter.ressel@fbh-berlin.de (P.R.); max.schiemangk@fbh-berlin.de (M.S.); andreas.wicht@fbh-berlin.de (A.W.); guenther.traenkle@fbh-berlin.de (G.T.)

[3]   Institute of Materials Science, Vietnam Academy of Science and Technology, 18 Hoang Quoc Viet, Cau Giay, Hanoi, Vietnam; tientq@ims.vast.ac.vn

*   Correspondence: phuong.nguyenthanh@hust.edu.vn; Tel.: +84-93-613-2266

check for updates

Abstract: The influence of the front facet reflectivity on the spectral linewidth of high power DFB (distributed feedback) diode lasers emitting at 780 nm has been investigated theoretically and experimentally. Characterization of lasers at various front facet reflections showed substantial reduction of the linewidth. This behavior is in reasonable agreement with simulation results. A minimum linewidth of 8 kHz was achieved at an output power of 85 mW with the laser featuring a front facet reflectivity of 30%. The device with a front facet reflectivity of 5% reached the same linewidth value at an output power of 290 mW.

1. Introduction

Narrow-linewidth lasers emitting in the range of 780 nm are suitable sources for atomic spectroscopy, atomic clocks, and Doppler laser cooling, particularly in space missions [1–4]. There are several approaches to generate narrow-linewidth laser emission in this wavelength region. In Reference [5], a laser output power of 11 W with sub 10 kHz linewidth at 780 nm had been achieved by using a second harmonic generation setup consisting of a fiber laser and a periodically-poled lithium niobate (PPLN) crystal. A Ti:Sapphire tunable laser is able to generate 8 W in the 750–810 nm region with a kHz linewidth [6]. An external wavelength stabilized ridge waveguide diode laser utilizing a volume holographic Bragg grating produced a maximum output power of 380 mW with 18 kHz linewidth (FWHM) [7]. However, there is a demand for miniaturized 780 nm laser systems at high output power with narrow spectral linewidth, which cannot be fulfilled by the previously mentioned systems in terms of compactness and power consumption. Semiconductor-based distributed feedback (DFB) lasers with excellent spectral purity, high energy-conversion efficiency, high reliability, and large frequency modulation bandwidth are attractive candidates for this demand. Some previous studies on the performance of the lasers [8–10] had shown very promising results for application in quantum optics. Therefore, further development of this diode laser type needs to be done. The aim of this work was to look for the ultimate limits (regarding high optical output power and narrow spectral linewidth) that can be reached with a single-section DFB laser without external stabilization.

The influences of laser cavity and the coupling coefficient on the DFB diode laser linewidth have been carefully analyzed in previous studies [8]. A high power DFB diode laser with a linewidth of

11 kHz was reported in Reference [9]. However, in this paper only the aspect of internal laser structure optimization was discussed. The behavior of the spectral linewidth under a variation of the facet reflectivity has not been extensively investigated so far. An increased facet reflectivity impacts the linewidth of a DFB laser in several ways (compare Equation (1) in Reference [8]). First, it leads to a decrease of the threshold gain, the rate of spontaneous emission, and Petermann's K factor which results in a decreased linewidth. Additionally, the effective α-factor changes but not in a definite manner. Second, compared to a vanishing facet reflectivity, the impact of the phase of the grating at the facet has to be considered, which results in varying linewidths for otherwise identical devices. Third, the difference of the threshold gains of the longitudinal modes decreases which results in a decreased side-mode suppression ratio and, therefore an increased linewidth or in dynamically unstable behavior.

Therefore, it is worthwhile to study how the spectral linewidth of DFB diode lasers varies with the facet reflectivity, especially in the high power operation regime. Theoretical analyses of the relation between the spectral linewidth of DFB diode lasers and facet reflectivity have been presented in References [11–13]. However, these reports do not address a stable single-longitudinal-mode operation of DFB diode lasers. More detailed results were published in References [14]. This work analyzes DFB diode lasers operating at 1300 nm with an output power of a few mW. Theoretically, the results show that higher facet reflectivity leads to narrower spectral linewidth, but at the same time provides a smaller yield of the single-longitudinal-mode operation. The experimental characterization of DFB diode lasers showed that the spectral linewidth takes on its minimum value at a front facet reflectivity of about 5% (with the rear facet as cleaved). An investigation of DFB diode lasers operating at 1500 nm is presented in References [15]. In this paper, the linewidth increased by a factor of 1.6 when the front facet reflectivity was reduced from a value of 32% (for the uncoated facet) to about 5%. This result is not in agreement with the findings of References [14]. Therefore, further studies on the influence of the facet reflectivity on the spectral linewidth are required.

In this paper, we will present the new results of a spectral linewidth study with high power DFB diode lasers emitting in the 780 nm region. Theoretical simulations of external differential efficiency and linewidth power product vs. front facet reflectivity have been conducted. Furthermore, DFB diode lasers with the front facet reflectivity varying from R < 0.01% to 30% have been characterized experimentally. The laser linewidths were derived from measurements of the frequency noise power spectral density (PSD). Linewidth-power dependence of DFB diode lasers will be presented.

2. Laser Fabrication and Experimental Setup

All DFB diode lasers studied in this letter stem from the same wafer grown in two steps by the low pressure metal organic vapor phase epitaxy (MOVPE) [16]. In the first step the n-$Al_{0.53}Ga_{0.47}As$ cladding, 250 nm thick n-$Al_{0.50}Ga_{0.50}As$ waveguide, tensile-strained 14 nm $GaAs_{0.785}P_{0.115}$ active quantum well (QW), 250 nm p-$Al_{0.50}Ga_{0.50}As$ waveguide, and the first part (550 nm) of the p-$Al_{0.53}Ga_{0.47}As$ cladding were grown on the n-GaAs substrate. An InGaP/GaAsP/InGaP (90 nm/20 nm/20 nm) layer sequence completed the first growth. A second order grating was formed in this layer sequence by holographic photolithography and wet-chemical etching of the upper GaAsP and InGaP layers (duty cycle of the 2n order grating equals 0.25). After surface cleaning, in the second step the remainder of the p-$Al_{0.53}Ga_{0.47}As$ cladding and a p-GaAs contact layer were grown. A ridge waveguide (RW) with a 2.2 μm wide ridge was implemented to provide lateral optical confinement.

The cavity lengths of the DFB diode lasers were 3 mm. In order to quantitatively investigate the effect of the front facet reflectivity of 780 nm DFB diode lasers, in the high output power regime, the DFB diode lasers were prepared with front facet reflections of R < 0.01%, R = 5%, R = 10%, and R = 30%, respectively. First, the facets of the lasers have been made unreactive using ZnSe layers, which was described in [17]. Afterward, thin films of Al_2O_3 with appropriate thicknesses were used to coat the laser facets for reflections of less than 30%. An additional TiO_2 layer has been employed to obtain a reflectivity of 30%. Commercially available software [18] has been used to calculate the various

layer thicknesses. White-light reflectometry has been employed to determine the layer thicknesses actually achieved. The rear facets of the lasers were coated to obtain a reflection of approximately 95% using SiO_2/Ta_2O_5 quarter-wave stacks. All lasers were soldered with AuSn on 250 µm thick CuW submounts, which were then soldered on so-called C-mounts with PbSn.

In order to determine the laser linewidth, we carried out a self-delayed heterodyne measurement with each laser. The output beam of the DFB diode laser was collimated and guided through a Faraday isolator (Qioptiq DLI, Feldkirchen, Germany, 60 dB) to suppress parasitic optical feedback. Subsequently, the laser beam was injected into an interferometer n which, one arm carried a 2 km (physical length) fiber delay and an acousto-optic modulator (Intra-Action ATM-804DA2B) to frequency-shift the radiation by 78 MHz. The beat note signal was detected with a fast photodetector (New Focus 1554-B) with a 3-dB bandwidth of 12 GHz and was recorded with an RF-spectrum analyzer (FSW 26 by Rohde & Schwarz GmbH & Co. KG, Munich, Germany). For each of the measurements presented here, a data set of 100 ms was recorded with an IQ bandwidth of 150 MHz. A detailed description of the subsequent determination of the frequency noise PSD can be found in References [19]. Lastly, the laser's intrinsic linewidth was derived from the level of the white noise of the frequency noise PSD by multiplication with $\pi/2$.

3. Results and Discussion

Figure 1 shows the effect of front facet coating on the power-current (PI) characteristics at a mount temperature of 25 °C. Lasers with front facet coatings of R < 0.01% and R = 5% show linearly increasing output power from threshold current up to 500 mA. The higher reflectivity lasers, R = 10% and 30%, have nonlinear PI characteristics. Furthermore, the linear slope efficiency of the lasers decreases from 0.66 W/A (R < 0.01%) to 0.63 W/A (R = 5%), 0.58 W/A (R = 10%) and 0.37 W/A (R = 30%) because of the reduced transmission at the front facets. The output power at 500 mA ranges from 138 mW (R = 30%) to 290 mW (R < 0.01%). At high power operation, DFB diode lasers with front facet reflectivity above 5% show significant instabilities in the PI characteristics, which are most prominently emphasized by several kinks. This behavior is most clearly observed for the device with R = 30% above an injection current of 300 mA.
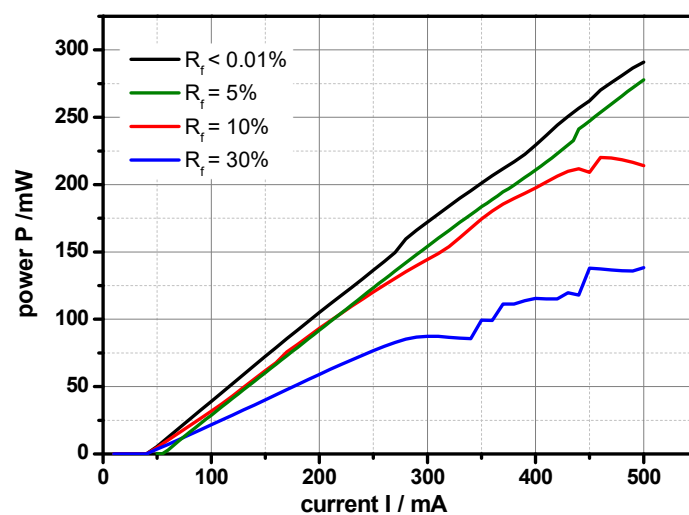

Figure 1. Power-current characteristics of 3 mm long 780 nm DFB (distributed feedback) diode lasers having different front facet reflections between R < 0.01% (black), 5% (green), 10% (red), and 30% (blue).

As theoretically shown, DFB lasers can exhibit different types of dynamical instabilities like pitchfork bifurcation [20], bistability [20] and self-pulsations [21,22]. All of these instabilities are triggered by the dependence of the carrier density, the refractive index and the gain on the

photon density via stimulated recombination, which results in longitudinal spatial hole burning and non-uniform index and gain profiles in order for, another longitudinal mode to reach the threshold. Moreover, the higher the front facet reflectivity, the smaller the difference of the threshold gain of adjacent modes that favors instabilities [23]. This can result in nonlinear power-current characteristics as well as broadened optical spectra, which was observed experimentally.

In Figure 2, we present spectral mappings of the DFB diode lasers with various front facet reflections at 25 °C. The laser with R < 0.01% shows single-mode operation from 40 mA to 420 mA injection current. Except for one mode hop, the laser with 5% front facet reflectivity operates in a single-mode in the range from 40 mA to 500 mA. The kinks in the power-current characteristics that can be observed for lasers with higher front facet reflections are related to regions of broad optical spectra visible in Figure 2c,d, which indicates a dynamically unstable behavior. The wavelength shift vs. the injection current is very similar for all devices with values of $\Delta\lambda/\Delta I$ in the range between 1.1 pm/mA and 1.6 pm/mA.
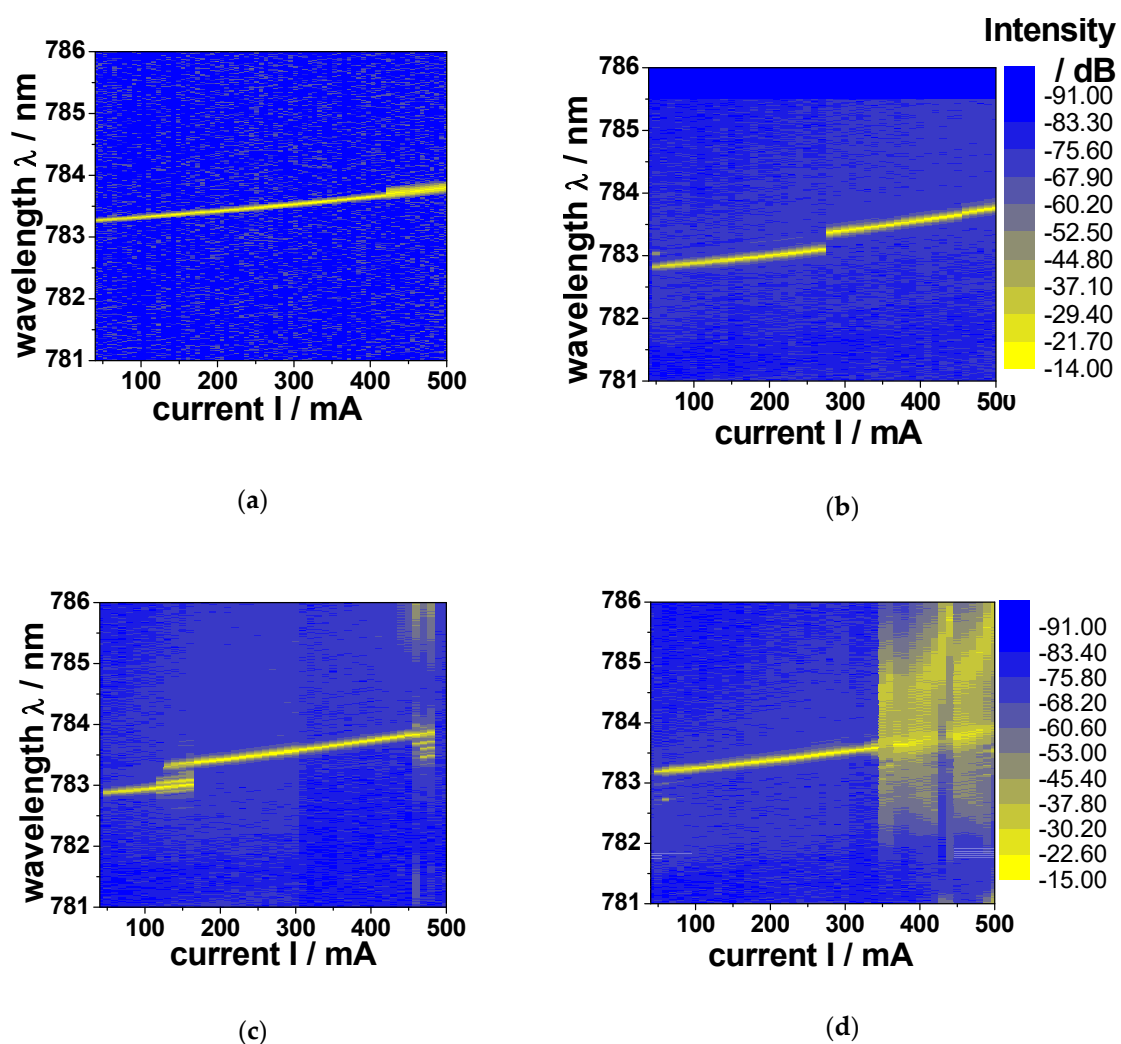
Figure 2. Spectral mappings of 780 nm DFB diode lasers with different front facet reflections: R < 0.01% (**a**), R = 5% (**b**), R = 10% (**c**), and R = 30% (**d**).

From the optical spectra we identified the regions of single-mode operation for the investigation of the linewidth. Figure 3 shows the frequency noise PSD of the self-delayed heterodyne beat note signal for each of the lasers when operated at an output power of 85 mW. At this output power, the intrinsic linewidth decreases from 28 kHz to 20 kHz, 14 kHz, and 8 kHz when the front facet reflection increases.
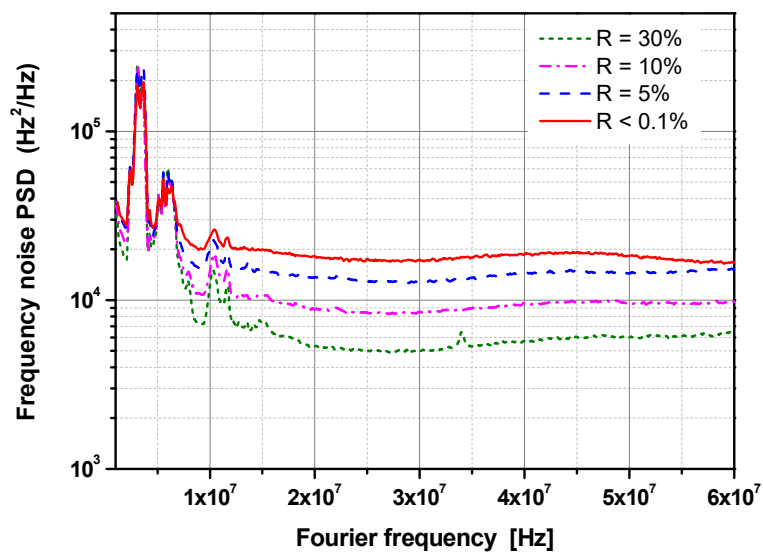
Figure 3. Frequency noise PSD (power spectral density) of the laser beat note signal in a self-delayed heterodyne setup at 85 mW output power for lasers with various front facet reflection: R < 0.01% (red solid); R = 5% (blue dashed); R = 10% (pink dot-dashed); and R = 30% (green short dashed).

The intrinsic linewidths of all lasers were investigated along with the injection current within their single-mode operation ranges. Figure 4 shows the linewidths of the DFB diode lasers vs. output power, which was calculated from the P-I characteristics (Figure 1). The device with R < 0.01% shows a linewidth reduction from 128 kHz at 20 mW to a value of 25 kHz at 98 mW (factor of 5.1 for a power ratio of 4.9). In the same power region, the device with R = 5% has a linewidth of 63 kHz at 24 mW and 19 kHz at 97 mW (linewidth reduction by a factor of 3.3 for a power ratio of 4.0). The linewidth of the laser with 10% front facet reflectivity reduces from 49 kHz at 22 mW to 14 kHz at 83 mW. This corresponds to a linewidth reduction ratio of 3.4 for a power ratio of 3.7. In the range from 38 mW to 72 mW, the laser with l0% front facet reflectivity shows a multi-mode operation (corresponding to injection currents from 110 mA to 170 mA, see Figure 2c). For this reason, the spectral linewidth of the device was not evaluated in this range. The laser with 30% reflectivity was investigated from 24 mW to 86 mW output power and exhibited linewidths of 27 kHz and 8 kHz, respectively. The linewidth reduction factor in this case is 3.4 (power ratio 3.6). By fitting the results with a 1/P dependence, we get the linewidth power products 2274 Hz·W (for R < 0.01%), 1574 Hz·W (for R = 5%), 1014 Hz·W (for R = 10%), and 659 Hz·W (for R = 30%).

As can be seen in the inset of Figure 4, the lasers with R = 5% and R = 10% reach the same linewidth at their highest single-mode operation injection currents. The device with R = 5% reaches the linewidth of 8 kHz at an output power of 290 mW and the other one at an output power of 215 mW. With increasing power, the linewidth of the laser with R < 0.01% continues to reduce to 17 kHz at 240 mW output power.

To explain the influence of the front facet reflection on the electro-optical properties as well as the spectral linewidth, we calculated the external differential efficiency and the linewidth power product of the lasers according to References [24,25]. The calculation was performed in three steps. First the carrier-density dependent part of the complex dielectric function and the rate of spontaneous emission of the GaAsP QW was calculated as a function of carrier density and wavelength using an 8 × 8 kp band model as described in References [26] and the results are stored in a look-up table. The imaginary part of the dielectric function gives the optical gain. The ratio of the derivatives of the real and imaginary parts of the dielectric function with respect to the carrier density is the linewidth enhancement factor [24]. In the second step the complex waveguide equation and a lateral diffusion equation were solved for the given applied voltage, power and wavelength, using the look-up table

created in the first step. The results such as injection current, effective index, modal gain and functions needed to calculate the spectral linewidth are stored in a table. Lastly, the electro-optical characteristics as well as the spectral linewidth are calculated by solving the coupled wave equations using the look-up table generated in the second step [25]. In this way, both lateral and longitudinal spatial hole burning have been taken into account.
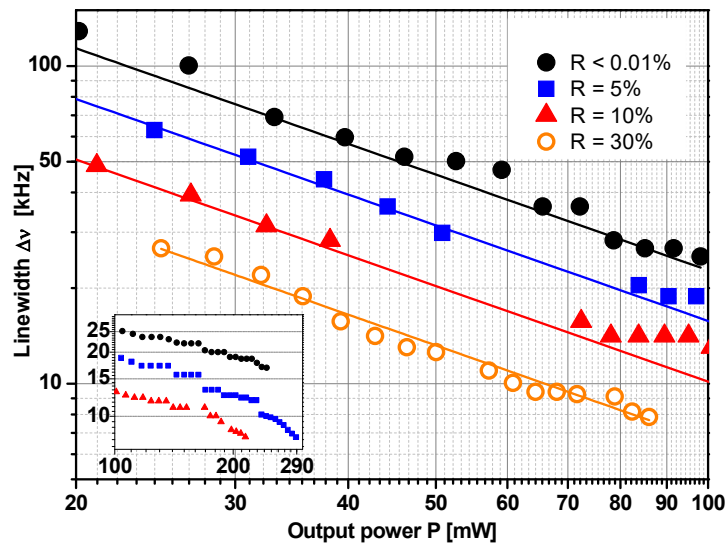

Figure 4. Dependence of the intrinsic linewidth on the output power for the DFB diode lasers with various front facet reflections: R < 0.01% (black solid circle), R = 5% (blue solid square), R = 10% (red solid triangle), and R = 30% (orange open circle). The solid lines show the result of fitting a 1/P dependence to the data. Inset: Linewidth vs. output power in the high power regime.

The parameters used in the simulation have been largely taken from Reference [27]. A summary of the most important parameters is given in Table 1. The reflection coefficient of the rear facet was set to 95%. The front facet reflections were 0.0001%, 5%, 10%, and 30%. The simulation scheme sketched above includes the dependence of effective linewidth enhancement, population inversion and the Petermann *K* factors on the reflections at the front facet and the phases of the grating at the rear and front facets. To compare with the experimental results the grating (or facet) phases have been varied between 0 and 2π. The minimum and maximum values of the external differential efficiency and the spectral linewidth due to a spontaneous emission noise at an output power of 50 mW have been determined [28].

Table 1. Summary of important parameters used in the simulation. QW: quantum well.

| Parameter	Unit	Value
thickness QW	nm	14
confinement factor QW		0.018
hole mobility QW	cm^2/Vs	170
effective phase index		3.3
effective group index		3.9
ridge width	μm	2.2
effective index step		5×10^{-3}
total series resistance of *p*-doped layers and *p*-contact	$\Omega \, cm^2$	7×10^{-5}
spreading resistance of *p*-doped layers	Ω	1.6×10^4
coupling coefficient	cm^{-1}	2
internal optical losses	cm^{-1}	5

Figure 5 presents the minimum and maximum simulation values of the external differential efficiency η_{diff} of the 780 nm DFB diode lasers. The experimental results of η_{diff} calculated from the power-current characteristics in Figure 1 (0.41, 0.40, 0.36, and 0.23) lie almost within the area of the simulation results, which shows that the coupling coefficient and the internal losses have been properly chosen. The external differential efficiency determined experimentally at the lowest facet reflectivity (corresponding to the highest out coupling losses) is smaller than predicted by the theory. A possible reason is the accumulation of carriers outside the active region not contributing to stimulated emission. This effect not taken into account in the simulation reduces the external differential efficiency.
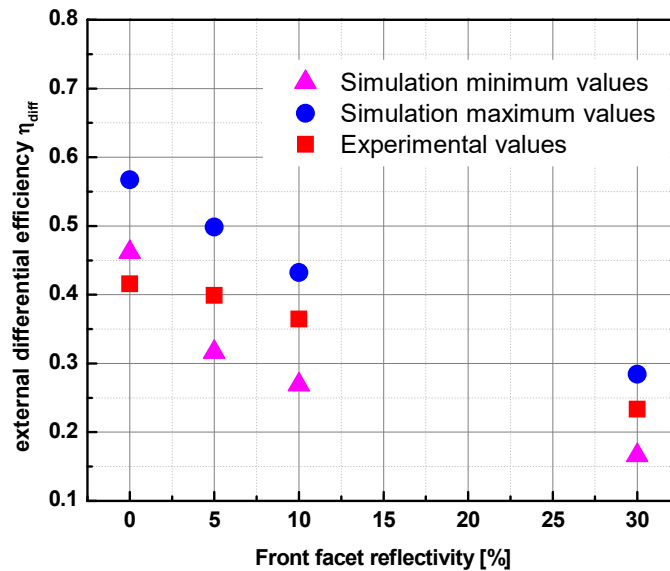
Figure 5. External differential efficiency of 780 nm DFB diode laser at 50 mW output power vs. front facet reflectivity: Minimum simulation values (pink solid triangle), maximum simulation values (blue solid circle), and experimental values (red solid square).

The experimental and the calculated minimum and maximum linewidth power products of the 780 nm DFB diode lasers are shown in Figure 6. The tendency of the experimental linewidth power products agrees with the theoretical prediction. The measured linewidth power product for the lowest front facet coating laser lies between the minimum and maximum simulated values. However, the theory predicts a much steeper drop of the linewidth with an increasing front facet reflection than experimentally observed. We should mention that in the theory we neglected other contributions to the intrinsic linewidth such as those due to fluctuations of the carrier density and of the profile shape of the photon density which should not strongly depend on the feedback strength. However, there is one contribution that rises with a decreasing side-mode suppression ratio due to an increased facet reflectivity, which is the impact of non-vanishing side modes on the linewidth of the main mode that could result in linewidth rebroadening [29]. We assume that this effect could be the cause of the increased deviation between simulated and measured linewidth.

As the simulations reveal, the decrease of the intrinsic spectral linewidth by the increase of the front facet reflection is caused by a reduction of the spontaneous emission rate due to the reduction of the threshold gain (partially compensated by an increase of the population inversion factor), a decrease of the Petermann *K* factor due to the increase of the resonator quality [11,12], an increase of the number of photons in the cavity, and a slight decrease of the effective linewidth enhancement factor [25]. The influence of an increasing front facet reflectivity on the linewidth is quite similar to an increasing coupling strength (*KL*) which was studied experimentally in Reference [8,30].
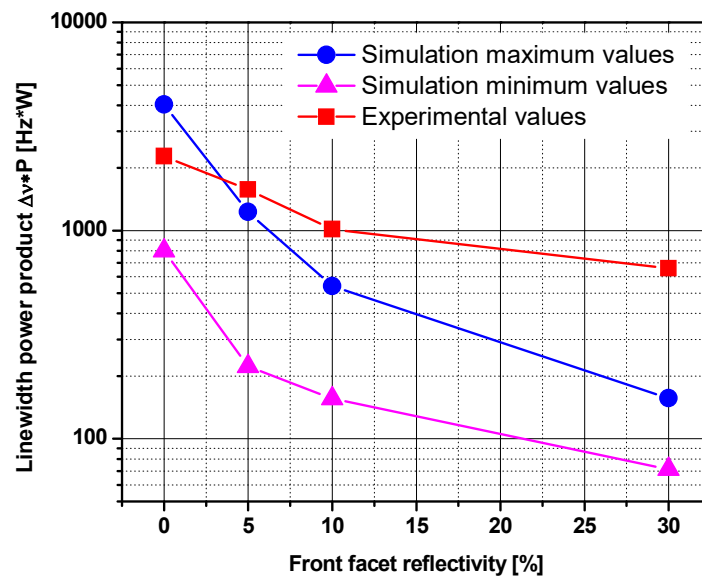
Figure 6. Linewidth power product of 780 nm DFB diode laser vs. front facet reflectivity: Minimum simulation values (pink solid triangle), maximum simulation values (blue solid circle), and experimental values (red solid square).

4. Conclusions

Within this paper, the influence of the front facet reflection on the electro-optical and linewidth properties of 780 nm DFB diode lasers has been investigated. The external differential efficiency is reduced from 0.41 to 0.23 when the AR coating varied from R < 0.01% to 30%. The linewidth power products are 2274 Hz·W, 1574 Hz·W, 1014 Hz·W, and 659 Hz·W for lasers with increasing reflection coefficient. A best intrinsic linewidth of 8 kHz was achieved for R = 5% at 290 mW, R = 10% at 215 mW, and R = 30% at 85 mW output power. Based on our knowledge this is the best performance reported so far for a solitary high power DFB diode laser in the 780-nm region. Furthermore, the findings of our analysis are beneficial for future optimization of semiconductor lasers aimed at applications which require both: narrow spectral linewidth and high optical output power.

References

1.　Herrmann, S.; Dittus, H.; Lämmerzahl, C. Testing the equivalence principle with atomic interferometry. *Class. Quantum Gravity* **2012**, *29*, 184003. [CrossRef]

2.　Camparo, J. The rubidium atomic clock and basic research. *Phys. Today* **2007**, *60*, 33–39. [CrossRef]

3.　Lienhart, F.; Boussen, S.; Carraz, O.; Zahzam, N.; Bidel, Y.; Bresson, A. Compact and robust laser system for rubidium laser cooling based on the frequency doubling of a fiber bench at 1560 nm. *Appl. Phys. B* **2007**, *89*, 177–180. [CrossRef]

4.　Hauth, M.; Freier, C.; Schkolnik, V.; Senger, A.; Schmidt, M.; Peters, A. First gravity measurements using the mobile atom interferometer GAIN. *Appl. Phys. B* **2013**, *113*, 49–55. [CrossRef]

5. Sane, S.S.; Bennetts, S.; Debs, J.E.; Kuhn, C.C.N.; McDonald, G.D.; Altin, P.A.; Close, J.D.; Robins, N.P. 11 W narrow linewidth laser source at 780 nm for laser cooling and manipulation of Rubidium. *Opt. Express* **2012**, *20*, 8915–8919. [CrossRef] [PubMed]

6. Chiow, S.; Herrmann, S.; Muller, H.; Chu, S. 6 W, 1 kHz linewidth, tunable continuous-wave near-infrared laser. *Opt. Express* **2009**, *17*, 5246–5250. [CrossRef] [PubMed]

7. Rauch, S.; Sacher, J. Compact Bragg grating stabilized ridge waveguide laser module with a power of 380 mW at 780 nm. *IEEE Photonics Technol. Lett.* **2015**, *27*, 1737–1740. [CrossRef]

8. Nguyen, T.-P.; Schiemangk, M.; Spießberger, S.; Wenzel, H.; Wicht, A.; Peters, A.; Erbert, G.; Tränkle, G. Optimization of 780 nm DFB diode lasers for high-power narrow linewidth emission. *Appl. Phys. B* **2012**, *108*, 767–771. [CrossRef]

9. Brox, O.; Bugge, F.; Mogilatenko, A.; Luvsandamdin, E.; Wicht, A.; Wenzel, H.; Erbert, G. Distributed feedback lasers in the 760 to 810 nm range and epitaxial grating design. *Semicond. Sci. Technol.* **2014**, *29*, 095018. [CrossRef]

10. Virtanen, H.; Uusitalo, T.; Karjalainen, M.; Ranta, S.; Viheriälä, J.; Dumitrescu, M. Narrow-Linewidth 780-nm DFB Lasers Fabricated Using Nanoimprint Lithography. *IEEE Photonics Technol. Lett.* **2018**, *30*, 51–51. [CrossRef]

11. Kojima, K.; Kyuma, K. Analysis of the spectral linewidth of distributed feedback laser diodes using the Green's function method. *Jpn. J. Appl. Phys.* **1988**, *27*, L1721–L1723. [CrossRef]

12. Agrawal, G.P.; Dutta, N.K.; Anthony, P.J. Linewidth of distributed feedback semiconductor lasers with partially reflecting Facet. *Appl. Phys. Lett.* **1986**, *48*, 457–459. [CrossRef]

13. Adams, M.; Henning, I.D. Linewidth calculations for distributed-feedback lasers. *IEE Proc. J. Optoelectron.* **1985**, *132*, 136–139. [CrossRef]

14. Ogita, S.; Hirano, M.; Soda, H.; Yano, M.; Ishikawa, H. Dependence of spectral linewidth of DFB lasers on facet reflectivity. *IEEE Electron. Lett.* **1987**, *23*, 347–349. [CrossRef]

15. Eddolls, D.V.; Park, C.A.; Buus, J. Dependence of Mode Stability and Linewidth of DFB Lasers on Facet Reflectivity and Coupling Coefficient. *IEEE Electron. Lett.* **1991**, *27*, 590–592. [CrossRef]

16. Wenzel, H.; Klehr, A.; Braun, M.; Bugge, F.; Erbert, G.; Fricke, J.; Knauer, A.; Weyers, M.; Tränkle, G. High-power 783 nm distributed-feedback laser. *IEEE Electron. Lett.* **2004**, *40*, 123–124. [CrossRef]

17. Ressel, P.; Erbert, G.; Zeimer, U.; Häusler, K.; Beister, G.; Sumpf, B.; Klehr, A.; Tränkle, G. Novel Passivation Process for the Mirror Facets of Al-Free Active-Region High-Power Semiconductor Diode Lasers. *IEEE Photonics Technol. Lett.* **2005**, *17*, 962–964. [CrossRef]

18. Essential McLeod. Available online: http://www.thinfilmcenter.com/essential.php (accessed on 15 May 2018).

19. Schiemangk, M.; Spießberger, S.; Wicht, A.; Erbert, G.; Tränkle, G.; Peters, A. Accurate frequency noise measurement of free-running lasers. *Appl. Opt.* **2014**, *53*, 7138–7143. [CrossRef] [PubMed]

20. Olesen, H.; Tromborg, B.; Pan, X.; Lassen, H.E. Stability and dynamic properties of multi-electrode laser diodes using a Green's function approach. *IEEE J. Quantum Electron.* **1993**, *29*, 2282–2301. [CrossRef]

21. Lowery, A.J. Dynamics of SHB-induced mode instabilities in uniform DFB semiconductor lasers. *IEEE Electron. Lett.* **1993**, *29*, 1852–1854. [CrossRef]

22. Marcenac, D.D.; Carroll, J.E. Distinction between multimoded and singlemoded self-pulsations-in DFB lasers. *IEEE Electron. Lett.* **1994**, *30*, 1137–1138. [CrossRef]

23. Radziunas, M.; Tronciu, V.Z.; Luvsandamdin, E.; Kürbis, C.; Wicht, A.; Wenzel, H. Study of microintegrated external-cavity diode lasers: Simulations, analysis, and experiments. *IEEE J. Quantum Electron.* **2015**, *51*, 1–8. [CrossRef]

24. Henry, C.H. Theory of the linewidth of semiconductor lasers. *IEEE J. Quantum Electron.* **1982**, *18*, 259–264. [CrossRef]

25. Wünsche, H.J.; Bandelow, U.; Wenzel, H. Calculation of Combined Lateral and Longitudinal Spatial Hole Burning in λ/4 Shifted DFB Lasers. *IEEE J. Quantum Electron.* **1993**, *29*, 1751–1761. [CrossRef]

26. Wenzel, H.; Erbert, G.; Enders, P. Improved theory of the refractive-index change in quantum-well lasers. *IEEE J. Sel. Top. Quantum Electron.* **1999**, *5*, 637–642. [CrossRef]

27. Piprek, J. *Semiconductor Optoelectronic Devices: Introduction to Physics and Simulation*, 1st ed.; Academic Press: San Diego, CA, USA, 2013; eBook ISBN 978-0-08-046978-2, Hardcover ISBN 978-0-12-557190-6.

28. Wenzel, H.; Klehr, A.; Braun, M.; Bugge, F.; Erbert, G.; Fricke, J.; Knauer, A.; Ressel, P.; Sumpf, B.; Weyers, M.; et al. Design and Realization of High-Power DFB Lasers. In Proceedings of the SPIE Physics and Applications of Optoelectronic Devices, Philadelphia, PA, USA, 25–28 October 2004; Volume 5594, pp. 110–123. [CrossRef]

29. Pan, X.; Tromborg, B.; Olesen, H. Linewidth rebroadening in DFB lasers due to weak side modes. *IEEE Photonics Technol. Lett.* **1991**, *3*, 112–114. [CrossRef]

30. Kihara, K.; Soda, H.; Ishikawa, H.; Imai, H. Evaluation of the coupling coefficient of a distributed feedback laser with residual facet reflectivity. *J. Appl. Phys.* **1987**, *62*, 1526–1527. [CrossRef]